

# Open Problems in Understanding the Nuclear Chirality

Jie Meng<sup>1,2,3</sup>, S.Q. Zhang<sup>2</sup>

<sup>1</sup> School of Physics and Nuclear Energy Engineering, Beihang University, Beijing 100191, China

<sup>2</sup> School of Physics and State Key Laboratory of Nuclear Physics and Technology, Peking University, 100871 Beijing, China

<sup>3</sup> Department of Physics, University of Stellenbosch, Stellenbosch, South Africa

E-mail: mengj@pku.edu.cn

**Abstract.** Open problems in the interpretation of the observed pair of near degenerate  $\Delta I = 1$  bands with the same parity as the chiral doublet bands are discussed. The ambiguities for the existing fingerprints of the chirality in atomic nuclei and problems in existing theory are discussed, including the description of quantum tunneling in the mean field approximation as well as the deformation, core polarization and configuration of particle rotor model (PRM). Future developments of the theoretical approach are prospected.

PACS numbers: 21.60.Ev, 21.60.Jz, 21.10.Re, 23.20.Lv

*Keywords:* Particle rotor model, Tilted axis cranking, nuclear chirality, microscopic theory

Submitted to: “*Focus issue on Open Problems in Nuclear Structure*”, *Journal of Physics G*

Handedness or chirality is a subject of general interests in molecular physics, elementary particles, and optical physics. The occurrence of chirality in nuclear physics was originally suggested in 1997 by Frauendorf and Meng in particle-rotor model (PRM) and tilted axis cranking (TAC) approach for triaxially deformed nuclei [1]. Since then, lots of experimental [2, 3, 4, 5, 6, 7, 8, 9, 10, 11, 12, 13, 14, 15, 16, 18, 19, 20, 21, 22, 23, 24, 25, 26, 27, 28, 29, 30, 31, 32, 33] as well as theoretical efforts [34, 35, 36, 37, 38, 39, 40, 41, 42, 43, 44, 45, 46, 47, 48, 49, 50, 51, 52, 53, 54, 55] have been devoted to search for nuclear chirality. With the near degenerate doublet bands reported in  $_{55}\text{Cs}$ ,  $_{57}\text{La}$ ,  $_{59}\text{Pr}$  and  $_{61}\text{Pm}$   $N = 75$  isotones, an island of chiral rotation was suggested in the  $A \sim 130$  mass region [2]. Up to now, candidate chiral doublet bands have been proposed in a number of odd-odd, odd- $A$  or even-even nuclei in the  $A \sim 100, 130, 190$  mass regions, for a review, see e.g. Ref. [56].

The best known examples for chiral doublet bands include  $^{126,128}\text{Cs}$  [12, 30],  $^{106}\text{Rh}$  [14] and  $^{135}\text{Nd}$  [20], which can be interpreted excellently with the PRM [44, 45, 46]. However, a paradox exists in interpreting a few doublet bands in terms of nuclear chirality such as  $^{134}\text{Pr}$  [28, 29] and  $^{106}\text{Ag}$  [16], which stimulates the present investigation.

## 1. Nuclear Chirality

The spontaneous broken of chiral symmetry is expected to occur in an atomic nucleus with a triaxial shape as well as a few high- $j$  valence particles and a few high- $j$  valence holes. For a triaxially deformed rotational nucleus, the collective angular momentum favors alignment along the intermediate axis, which in this case has the largest moment of inertia, while the angular momentum vectors of the valence particles (holes) favor alignment along the nuclear short (long) axis. The three mutually perpendicular angular momenta can be arranged to form two systems with opposite chirality, namely left- and right-handedness, see Fig. 1 for a schematic illustration. These two systems are transformed into each other by the chiral operator which combines time reversal and spatial rotation of  $180^\circ$ ,  $\chi = \mathcal{TR}(\pi)$ . The spontaneous breaking of chiral symmetry thus happens in the body-fixed reference frame. In the laboratory reference frame, with the restoration of chiral symmetry due to quantum tunneling, the so-called chiral doublet bands, i.e., a pair of  $\Delta I = 1$  bands (normally regarded as near degenerate) with the same parity, are expected to be observed in triaxial nuclei.

### 1.1. Classic picture

This chiral picture is firstly proposed and illustrated theoretically in PRM and TAC approach [1].

TAC is the version of the mean field theory that permits the calculation of the orientation of the deformed density distribution relative to the (space-fixed) angular momentum vector. For the triaxial nuclei, as illustrated in Fig. 1, there exists the possibility of the aplanar solutions, where the angular momentum vector does not lie

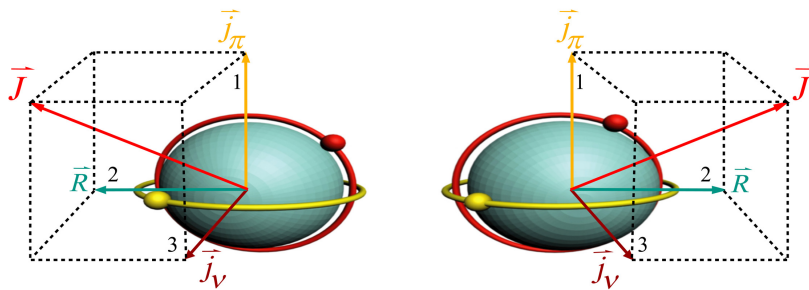


**Figure 1.** Left- and right-handed chiral systems for a triaxial odd-odd nucleus.

in one of the principle planes defined by the principal axes of the deformed density distribution. Due to the invariance of the intrinsic deformed density distribution with the rotations  $\mathcal{R}_1(\pi), \mathcal{R}_2(\pi), \mathcal{R}_3(\pi)$  ( $D_2$  symmetry), the aplanar TAC solutions are restricted in two of eight octants of principle axes frame, i.e., the first octant (right-handed) and the fourth octant (left-handed) shown in Fig. 1. These two aplanar solutions are chiral as they cannot be transformed into each other by a rotation, but degenerate as TAC is a semi-classic model which cannot describe the quantum tunneling between the left-handed and right-handed states [1].

The mean field version of the TAC adopted in Ref. [1] is the simple single- $j$  model. With a hybrid potential combining the spherical Woods-Saxon single-particle energies and the deformed part of the Nilsson potential, chiral rotation has been studied by the Strutinsky shell correction TAC (SCTAC) method [35, 36]. More microscopically, the self-consistent Skyrme Hartree-Fock cranking model has been developed and provides chiral solutions in  $N = 75$  isotones [37, 38]. The cranked relativistic mean field (RMF) theory has been reported only in the contexts of principle axis rotation [57, 58] and planar rotation [59, 60]. The generalization thereof for searching for chiral solutions, i.e., the aplanar rotation, is still under development.

The advantage of the cranked mean field approach is that it can be easily extended to the multi-quasiparticle case. However, the usual cranking approach is a semiclassical model, where the total angular momentum is not a good quantum number, and the description of quantum tunneling of chiral partners is beyond the mean field approximation [34].

### 1.2. Quantum picture

PRM is a quantum model consisting of the collective rotation and the intrinsic single-particle motions, in which the total Hamiltonian are diagonalized with total angular momentum as a good quantum number. The PRM describes a system in the laboratory reference frame in which the spontaneous broken chiral symmetry in intrinsic reference frame has been restored. The energy splitting and quantum tunneling between doublet bands can be obtained directly. By analyzing the orientations of the angular momenta for the rotor as well as the valence proton and neutron, and the effective angles between

these angular momenta, the chiral geometry represented by a remarkable and similar aplanar rotation between doublet bands can be revealed in a quantum way [43, 45, 19].

Chirality for nuclei in  $A \sim 100$  and  $A \sim 130$  regions has been studied with the particle-rotor model [40, 41], or the core-quasiparticle/core-particle-hole coupling model [8, 9] by following the Kerman-Klein-Dönau-Frauendorf method [61]. With the pairing correlations taken into account to simulate the configurations of multi-particles sitting in a high  $j$ -shell, PRM with a quasi-proton and a quasi-neutron coupled with a triaxial rotor has been applied to study chiral doublet bands [43, 44]. The (quasi-)particle rotor model can well describe all the energy spectra and the ratios  $B(M1)/B(E2)$  and  $B(M1)_{\text{in}}/B(M1)_{\text{out}}$  of chiral bands for most nuclei, for example  $^{126}\text{Cs}$  in  $A \sim 130$  [44],  $^{106}\text{Rh}$  in  $A \sim 100$  [45], and  $^{198}\text{Tl}$  in  $A \sim 190$  mass region [19]. Recently, a triaxial  $n$ -particle- $n$ -hole PRM to treat more than one valence proton and one valence neutron has been developed and applied to the study of nuclear chirality in  $^{135}\text{Nd}$  with the  $2p1n$  configuration  $\pi h_{11/2}^2 \otimes \nu h_{11/2}^{-1}$  [46].

Although the particle rotor model has been applied to investigate the nuclear chirality extensively, it is a phenomenological model based on a rigid triaxially deformed core. The quadrupole deformation parameters  $\beta$  and  $\gamma$  as well as the particle-hole configuration are imposed from the beginning. Therefore, the response of the deformation and triaxiality with the nuclear rotation as well as their influence on chirality are beyond the current version of PRM.

## 2. Rigidity of Finite Many-Body System

### 2.1. Stable $\gamma$ deformation

By means of PRM with stable  $\gamma$  deformation, it has been demonstrated that for the symmetric particle-hole configuration such as  $\pi h_{11/2} \otimes \nu h_{11/2}^{-1}$  in  $A \sim 130$  region and  $\pi h_{9/2} \otimes \nu h_{9/2}^{-1}$  in  $A \sim 80$  region, the best condition for the appearance of the chiral doublet bands is the maximum triaxiality  $\gamma = 30^\circ$ , while for the asymmetric particle-hole configuration such as  $\pi g_{9/2}^{-1} \otimes \nu h_{11/2}$  in  $A \sim 100$  region, the best condition deviates the maximum triaxiality to  $\gamma \sim 27^\circ$  [40, 41]. Generally speaking, the chiral doublet bands are expected in the interval  $20^\circ \leq \gamma \leq 40^\circ$  for PRM with particle-hole configuration .

For PRM with quasi-particle configurations, further investigation has verified that the chiral geometry holds for the same deformation interval  $20^\circ \leq \gamma \leq 40^\circ$  [43, 46]. However, the deviation of the shape from  $\gamma = 30^\circ$  or the configuration from pure particle-hole case will retrogress the level degeneracy and prefer a near constant energy difference between doublet bands.

Naturally, one must go beyond the limit of rigid  $\gamma$  deformation in the future study of the nuclear chirality. The potential energy surface in  $(\beta, \gamma)$  plane in the microscopic mean field calculations including the triaxial degree of freedom will provide hints on these issues.

## 2.2. Shape coexistence and $M\chi D$

The adiabatic and configuration-fixed constrained triaxial RMF approaches were developed and applied to  $^{106}\text{Rh}$  [53]. The triaxial shape coexistence as well as the  $\beta$  and  $\gamma$  deformation suitable for chirality were found. Based on the triaxial deformations and their corresponding high- $j$  proton-hole and neutron-particle configurations, the possible existence of more than one pair of chiral bands in one single nucleus — multiple chiral bands ( $M\chi D$ ) — is suggested in  $^{106}\text{Rh}$ . Such investigation has been extended to the rhodium isotopes and the existence of  $M\chi D$  is suggested in  $^{104,106,108,110}\text{Rh}$  [54]. The investigation provides not only further support for the prediction of  $M\chi D$  in  $^{106}\text{Rh}$ , but also presents new experimental opportunity for the observation of  $M\chi D$  in  $A \sim 100$  mass region.

The prediction of  $M\chi D$  [53, 54] has been further examined by including time-odd fields [55]. The configuration-fixed constrained triaxial relativistic mean-field approach including time-odd fields has been applied to study the candidate  $M\chi D$  nucleus  $^{106}\text{Rh}$ . The calculations support the previous prediction of the  $M\chi D$ , although the time-odd fields contribute 0.1-0.3MeV to the total energy and slightly modify the  $\beta$  and  $\gamma$  deformation.

So far in the constraint RMF calculations, the rotational degree of freedom is switched off. In order to include the rotational degree of freedom in microscopic energy density functional theories self-consistently, the three-dimensional cranking or even angular momentum projection techniques should be applied and the deformation should be obtained by minimizing the energy for given total angular momentum, which is still quite challenging even for modern advanced computational facilities.

## 2.3. Deformation response to rotation

Total Routhian surface (TRS) calculations are often used to track the deformation variation with rotation. The idea of the TRS is to search for the energy minimum in the deformation space for a given rotational frequency. Based on the Nilsson or the Woods-Saxon phenomenological potentials and the Strutinsky shell correction method, TRS calculations are mostly restricted to the principle axis cranking only. Its extension for tilted axis cranking is simple in idea but quite difficult in practice, i.e., for a given cranking rotation frequency  $\hbar\omega$  with the tilted angles  $(\theta, \varphi)$ , the deformations  $(\beta, \gamma)$  are firstly obtained by minimizing the TRS, then this procedure should be repeated for all tilted angles  $(\theta, \varphi)$  and finally the TRS should be minimized with  $(\theta, \varphi)$ . In such a way, the deformation and the tilted angles as a function of the rotation frequency can be obtained.

In comparison, the corresponding microscopic calculations based on modern energy density functionals have the advantage that the deformations  $(\beta, \gamma)$  are self-consistently obtained for a given cranking rotation frequency  $\hbar\omega$  with the tilted angles  $(\theta, \varphi)$  and one needs only minimizing the TRS with  $(\theta, \varphi)$ . However, the self-consistent microscopic iteration can be quite time consuming. So far such calculations have been realized for

conventional energy density functionals [37, 38] and covariant energy density functionals in two dimensions [59, 60].

#### 2.4. Coupling between vibration and rotation

For finite many-body systems such as the atomic nucleus, the deformation may never be rigid but more or less soft. Naturally in PRM, one may consider the vibration degree of freedom of the core in addition to the collective rotation, i.e., the collective vibration-rotation model [62].

Taking such a collective vibration-rotation model, the calculated results for the rigid or the  $\gamma$ -unstable core are qualitatively very similar for an odd-odd nucleus [52]. Similarly, describing the core by the Interacting Boson Model (IBM) with O(6) dynamical symmetry [49], the chiral bands have been investigated and the dynamic chirality with shape fluctuation is proposed.

### 3. Fingerprints for Nuclear Chirality

#### 3.1. Energy spectra

Since the prediction of the chirality in atomic nuclei [1], the appearance of a pair of near degenerate  $\Delta I = 1$  bands with the same parity has been taken as its fingerprint. Of course, the definition of the “near degenerate” is subjective. Furthermore, it should be emphasized that the experimental signals suggested as the fingerprints of the nuclear chirality are essentially based on one particle and one hole coupled to a rigid triaxial rotor with  $\gamma = 30^\circ$  [1, 42, 17]. The “near degenerate” depends on the deformation, valent nucleon configuration, and their couplings. Normally, the observed “near degenerate” energy is around 200 keV.

From the energy spectra, one can also extract other physical observables such as spin-alignment and the energy staggering parameter  $S(I) = [E(I) - E(I - 1)]/2I$  and use them as possible fingerprints. So far, most of the proposed chiral doublet candidates are mainly based on the observed near degenerate  $\Delta I = 1$  doublets bands.

A systematic explanation by excluding the chirality will be very difficult, if not impossible, for the observed chiral doublet candidates in more than 30 nuclei.

#### 3.2. Electromagnetic transitions

With more and more chiral doublet candidates proposed, it is quite natural to have observable fingerprints other than the energy spectra. The electromagnetic transition in doublet bands become a hot topic in identifying the chiral bands.

Based on the  $\pi h_{11/2} \otimes \nu h_{11/2}^{-1}$  configuration coupled to a rigid triaxial rotor with  $\gamma = 30^\circ$ , the selection rule for electromagnetic transitions in the chiral bands has been proposed [42], including the odd-even staggering of intraband  $B(M1)/B(E2)$  ratios and interband  $B(M1)$  values, as well as the vanishing of the interband  $B(E2)$  transitions at high spin region.

With the improvement of experimental techniques, lifetime measurements for the doublet bands have been done and the  $B(M1)$  and  $B(E2)$  transition probabilities are extracted [28, 30, 31, 32, 33] and examined against the fingerprints of the chiral doublet bands.

Similar as the case of the energy spectra, the fingerprints of the electromagnetic transition depend on the deformation, valent nucleon configuration, and their couplings too. The dependence of these fingerprints on triaxiality have been investigated in PRM with  $\pi h_{11/2} \otimes \nu h_{11/2}^{-1}$  configuration [47]. It is found that the  $B(M1)$  staggering is associated strongly with the characters of nuclear chirality, i.e., the staggering is weak in chiral vibration region and strong in the static chirality region. This result also qualitatively agrees with the recent lifetime measurements for the doublet bands in  $^{128}\text{Cs}$  and  $^{135}\text{Nd}$ . The former was claimed as a good example revealing chiral symmetry breaking [30], where the pronounced  $B(M1)$  staggering is exhibited. The latter was suggested to reveal the chiral vibration motions for  $I < 41/2\hbar$  region [31], where the weak  $B(M1)$  staggering is shown.

Nevertheless, a model independent selection rule for electromagnetic transitions in the chiral bands is still missing.

### 3.3. Other fingerprints

Apart from energy spectra and electromagnetic transitions, the spin-alignment and the energy staggering parameter are also used in the discussion of the chiral pair bands. As the spin-alignment and the energy staggering parameter are extracted from the energy spectra, they inherit naturally the same uncertainty. Ideally, the spin alignments, moment of inertia, and electromagnetic transition probabilities are expected to be identical, or in practice very similar for chiral pair bands [29].

Examining against these criteria, the doublet bands of  $^{128}\text{Cs}$  have been regarded as the best known example for the chiral symmetry broken [30]. While the lifetime measurement performed for doublet bands in  $^{134}\text{Pr}$ , which had been considered as the best examples of chiral rotation due to their extremely small level discrepancy between the doublet bands, stirred quite a lot of debates on the interpretation of the chirality [28, 29]. Again, new and model independent fingerprints are highly demanded.

## 4. Interpretations Excluding Chiral Picture

Although candidate chiral doublet bands have been proposed in a number of odd-odd, odd- $A$  or even-even nuclei in the  $A \sim 100, 130, 190$  mass regions, their identification is mainly based on the observed energy spectra of doublet bands. Several competitive mechanisms have been proposed to explain the pair of near degenerate  $\Delta I = 1$  bands with the same parity.

#### 4.1. $\gamma$ band

In the collective vibration-rotation model, the so-called  $\gamma$ -band, which has been observed in many deformed nuclei, has the quantum numbers  $K = 2, n_\beta = 0, n_\gamma = 0$  and is built on the quantum mechanical zero point vibration in the  $\gamma$ -direction [62, 63]. For the doublet bands in Cs, La, Pr and Pm  $N = 75$  isotones [2], the interpretation of the yrare band as a  $\gamma$  vibration coupled to the yrast band has been ruled out because the  $\gamma$ -vibration energies in this mass region are  $\geq 0.60$  MeV, which can not explain the observed small energy displacement ( $< 0.40$  MeV). However, one can not rule out the interpretation of doublet bands in a  $\gamma$  vibration picture. Furthermore, the influence of the  $\gamma$  vibration on the chiral rotation should be treated more carefully.

#### 4.2. Shape coexistence

In order to explain the observed electromagnetic transitions for the doublet bands in  $^{134}\text{Pr}$  [28], the concept of shape coexistence has been proposed [29]. Based on a two-bands crossing model, a ratio around two for the transition quadrupole moments has been obtained for the doublet bands in  $^{134}\text{Pr}$  in the spin interval  $I = 14\text{--}18$  where the observed energies are almost degenerate, which implies a considerable difference in the nuclear shape associated with the two bands and thus the doublet bands in  $^{134}\text{Pr}$  cannot be interpreted as chiral bands [29].

To reproduce the observed near degenerate spectra and electromagnetic transitions in  $^{134}\text{Pr}$  with either the shape coexistence or the chiral picture in a microscopic and self-consistent way remains to be a challenge.

#### 4.3. Many particle correlations

In the framework of the projected shell model (PSM) with triaxial deformation, the doublet bands in  $^{134}\text{Pr}$  are investigated [64]. By reproducing the energy spectra, it is found that in the region  $I = 14$  to 18, the band 1 is a 2-quasi-particle state, e.g., of  $\pi h_{11/2}\nu h_{11/2}$  configuration, while the band 2 is mainly a 4-quasi-particle state, e.g., of  $\pi h_{11/2}d_{5/2}g_{7/2}\nu h_{11/2}$  configuration. Therefore many particle correlations was proposed as another possible mechanism of doublet bands in  $^{134}\text{Pr}$  [64]. It will be quite interesting to have more detailed and quantitative comparisons with the observed energy spectra,  $B(E2)$  and  $B(M1)$  values in order to figure out the role of the many particle correlations. In fact, the many particle correlations are also necessary to be taken into account in PRM study of the nuclear chirality.

#### 4.4. Pseudospin partner bands

The pseudospin symmetry [65, 66] in finite nuclei have been known as a relativistic symmetry and become of the hot topic in current nuclear physics frontiers [67, 68, 69, 70]. The concept of the pseudospin symmetry has been used in the interpretation of the identical bands observed in superdeformed nucleus [71].

Recently, pairs of  $\Delta I = 1$  doublet bands with the same parity and near degenerate energies have been observed in several odd-odd and odd- $A$  nuclei, e.g.,  $^{108}\text{Tc}$  [72],  $^{128}\text{Pr}$  [73],  $^{186}\text{Ir}$  [74], and  $^{195}\text{Pt}$  [75], and explained in terms of the coupling of a proton (neutron) and a neutron (proton) pseudospin doublet. Normally, the observed pseudospin doublet bands start at relatively lower spin and show the opposite odd-even phase in the  $B(M1)$  staggering between the partners, while the chiral doublet bands hold the same phase.

#### 4.5. Core polarization

The classic examples for chirality are triaxial odd-odd nuclei where the angular momenta of a high- $j$  particle and a high- $j$  hole are aligned along the short and long axis, respectively, and the angular momentum of collective rotation is aligned with the intermediate axis. The observation of doublet bands in odd- $A$  and even-even nuclei further exemplify the general geometric character of chiral symmetry breaking, because the non-planar rotation is related to more complicated particles and holes configuration.

Another interesting issue is the core polarization effect. In addition to the PRM and TAC approaches, the interacting boson fermi model [49, 50, 51] and the pair truncated shell model [48] have been applied to investigate the observed doublet bands as well. In comparison with the PRM with a rigid rotor, the quadrupole collective excitations of the even-even core are taken into account by the ingredients of the collective nucleon pairs with angular momenta of zero and two.

## 5. Microscopic Model Expected

### 5.1. Beyond TAC

Chiral rotation has been extensively studied by TAC method with a phenomenological Woods-Saxon or Nilsson potential, and the self-consistent Skyrme Hartree-Fock model. The advantage of the TAC is that it can be easily extended to the multi-quasiparticle case. However, the usual cranking approach is a semiclassical model, where the total angular momentum is not a good quantum number and the electromagnetic transitions are calculated in a semiclassical approximation. Furthermore, the description of nonlinear quantum tunneling of chiral partners is beyond the mean field approximation, as well as the random phase approximation in which the excitations of the equilibrium mean field are described as harmonic vibrations only.

Before the onset of chirality, the precursor of the symmetry breaking occurs as a soft vibration between the right- and left-handed configurations. These chiral vibrations have been studied in the framework of the random phase approximation (RPA) based on the TAC mean field [39, 31]. Currently, the RPA calculations are only limited on the TAC with a spherical Woods-Saxon potential for the mean field together with a QQ-force and a constant pair gap. Further investigation in a more microscopic way is expected. In particular, we need a model which could simultaneously describe the chiral

vibration dominated by a slow vibration, static chirality by the quantum tunneling, and the smooth transition from chiral vibration to static chirality.

### 5.2. Rotational symmetry restoration

Due to the mean field approximation, which is rooted in both shell models and microscopic approaches, the rotational symmetry has been broken in the deformed intrinsic reference frame. In order to restore the rotational symmetry, it is necessary to use the standard angular momentum projection (AMP) techniques [63].

In the late 1970s, Hara and Iwasaki applied AMP techniques and developed the projected shell model (PSM) to obtain the good angular momentum states from the Nilsson state [76, 77]. Later, the triaxiality has been taken into account and applied to study the yrast and  $\gamma$ -vibrational bands for both  $\gamma$ -soft and well-deformed nuclei [78, 79, 80]. In principle, the doublet bands in triaxial nuclei can be understood in the framework of PSM with triaxially deformed multi-quasiparticle states. Such calculation has been reported for  $^{134}\text{Pr}$ , where the partner bands have been suggested to have completely different configurations [64]. It will be very interesting to apply the PSM to study the chiral doublet candidates systemically and examine their detailed observables including the electromagnetic properties and the energy spectra.

Due to the numerical complexity, only recently it become possible to apply the AMP procedures for the microscopic energy density functional [81, 82, 83, 84, 85]. However, in these studies, the axial symmetry has been imposed from the beginning. Such restriction simplifies the numerical calculation considerably, because the integrals over two of the three Euler angles can be treated analytically and one is left with a one-dimensional numerical integration.

In the context of energy density functionals, a full three-dimensional angular momentum projection (3DAMP) has been performed with a simple Skyrme-type interaction [86], and the full Skyrme energy functional [87]. Only very recently, angular-momentum and particle-number projections with configuration mixing have been attempted in the context of the triaxial Hartree-Fock-Bogoliubov (HFB) theory with the full Skyrme energy functional [88]. On top of the triaxial relativistic mean-field calculations, a full three-dimensional angular momentum projection has been implemented [89], even with configuration mixing [90]. Although these modern recipes have been successfully applied to the light even-even nuclei like  $^{24}\text{Mg}$ , there is still a long way for their applications to chiral doublet candidates due to the configuration space and the quasi-particle excitations.

### 5.3. Collective Hamiltonian parameter

In this subsection, we would like to discuss the possibility for the PRM to include the vibration-rotation coupling in a microscopic way to study the nuclear chirality.

Recently, a new implementation is developed for the solution of the eigenvalue problem of a five-dimensional collective Hamiltonian for quadrupole vibrational and

rotational degrees of freedom, with parameters determined by constrained self-consistent relativistic mean-field calculations for triaxial shapes. The model is tested in a series of illustrative calculations of potential energy surfaces and the resulting collective excitation spectra and transition probabilities of the chain of even-even gadolinium [91], neodymium and samarium isotopes [92]. For neodymium and samarium isotopes, the first-order nuclear quantum phase transition has been demonstrated in the characteristic energy spectra thus obtained [92, 93].

The possible extension of the PRM is the replacement of the core by the collective Hamiltonian with the parameters extracted in a similar way, which may provide a new dimension in the description of the chiral doublet bands.

## 6. Summary

The spontaneous broken of chiral symmetry suggested in atomic nucleus one decade ago has attracted lots of attention both experimentally and theoretically. Several fingerprints of the chirality in atomic nuclei have been proposed although ambiguities still exist. Semi-classically or quantum mechanically, the phenomenological or microscopic model has achieved great success in prediction and the description of the chiral doublet bands. However, the interpretation of the experimentally observed doublet bands as chiral partners can be contradictory.

Theoretically, open problems in existing model are discussed, including the description of quantum tunneling in the mean field approximation as well as the deformation, core polarization and configuration of PRM. More efforts are needed in developing a model which could simultaneously describe the chiral vibration dominated by a slow vibration, static chirality by the quantum tunneling, and the smooth transition from chiral vibration to static chirality. With the rapid development of computing facilities, a full three-dimensional angular momentum projection on top of the triaxial relativistic mean-field calculations with quasi-particle excitation may be realized. Meanwhile the PRM can also be combined with the collective Hamiltonian with the parameters extracted in a microscopic way.

## Acknowledgments

The authors wish to thank Y.S. Chen, Z.C. Gao, Z.P. Li, B. Qi, F.R. Xu, J.M. Yao and S.G. Zhou for carefully reading the manuscript and useful discussions. This work is partly supported by the Major State Basic Research Developing Program 2007CB815000, the National Natural Science Foundation of China under Grant Nos. 10775004, 10975007, 10975008 and 10720003.

## References

- [1] S. Frauendorf and J. Meng, *Nucl. Phys. A* **617**, 131 (1997).
- [2] K. Starosta *et al.*, *Phys. Rev. Lett.* **86**, 971 (2001).

- [3] T. Koike, K. Starosta, C.J. Chiara, D.B. Fossan, and D.R. LaFosse, *Phys. Rev. C* **63**, 061304(R) (2001).
- [4] A. A. Hecht *et al.*, *Phys. Rev. C* **63**, 051302(R) (2001).
- [5] D. J. Hartley *et al.*, *Phys. Rev. C* **64**, 031304(R) (2001).
- [6] R. A. Bark, *et al.*, *Nucl. Phys. A* **691**, 577 (2001).
- [7] X. F. Li *et al.*, *Chin. Phys. Lett.* **19**, 1779 (2002).
- [8] K. Starosta *et al.*, *Phys. Rev. C* **65**, 044328 (2002).
- [9] T. Koike, K. Starosta, C. J. Chiara, D. B. Fossan, and D. R. LaFosse, *Phys. Rev. C* **67**, 044319 (2003).
- [10] G. Rainovski *et al.*, *Phys. Rev. C* **68**, 024318 (2003).
- [11] A. J. Simons *et al.*, *J. Phys. G* **31**, 541 (2005).
- [12] S. Y. Wang, Y. Z. Liu, T. Komatsubara, Y. J. Ma, and Y. H. Zhang, *Phys. Rev. C* **74**, 017302 (2006).
- [13] C. Vaman, D. B. Fossan, T. Koike, K. Starosta, I. Y. Lee and A. O. Macchiavelli, *Phys. Rev. Lett.* **92**, 032501 (2004).
- [14] P. Joshi *et al.*, *Phys. Lett. B* **595**, 135 (2004).
- [15] P. Joshi *et al.*, *Eur. Phys. J. A* **24**, 23 (2005).
- [16] P. Joshi, *et. al.*, *Phys. Rev. Lett.* **98**, 102501 (2007).
- [17] S. Y. Wang, S. Q. Zhang, B. Qi and J. Meng, *Chin. Phys. Lett.* **24**, 664 (2007).
- [18] D. L. Balabanski *et al.*, *Phys. Rev. C* **70**, 044305 (2004).
- [19] E. A. Lawrie, *et al.*, *Phys. Rev. C* **78**, 021305(R) (2008).
- [20] S. Zhu *et al.*, *Phys. Rev. Lett.* **91**, 132501 (2003).
- [21] J. A. Alcántara-Núñez *et al.*, *Phys. Rev. C* **69**, 024317 (2004).
- [22] J. Timár *et al.*, *Phys. Lett. B* **598**, 178 (2004).
- [23] J. Timár, *et al.*, *Phys. Rev. C* **73**, 011301(R) (2006).
- [24] Y. X. Zhao, *et al.*, *Chin. Phys. Lett.* **26**, 082301 (2009).
- [25] E. Mergel *et al.*, *Eur. Phys. J. A* **15**, 417 (2002).
- [26] S. J. Zhu, *et al.*, *Eur. Phys. J. A* **25**, (Suppl. 1) (2005) 459.
- [27] Y. X. Luo, *et al.*, *Phys. Lett. B* **670**, (2009) 307.
- [28] D. Tonev *et al.*, *Phys. Rev. Lett.* **96**, 052501 (2006).
- [29] C.M. Petrache, G.B. Hagemann, I. Hamamoto and K. Starosta, *Phys. Rev. Lett.* **96**, 112502 (2006).
- [30] E. Grodner *et al.*, *Phys. Rev. Lett.* **97**, 172501 (2006).
- [31] S. Mukhopadhyay *et al.*, *Phys. Rev. Lett.* **99**, 172501 (2007).
- [32] T. Suzuki *et al.*, *Phys. Rev. C* **78**, 031302(R) (2008).
- [33] L. L. Wang *et al.*, *Chin. Phys. C* **33**, Suppl.1, 173(2009).
- [34] S. Frauendorf, *Rev. Mod. Phys.* **73**, 463 (2001).
- [35] V. I. Dimitrov, S. Frauendorf and F. Dönau, *Phys. Rev. Lett.* **84**, 5732 (2000).
- [36] V. I. Dimitrov, F. Dönau and S. Frauendorf, *Phys. Rev. C* **62**, 024315 (2000).
- [37] P. Olbratowski, J. Dobazewski, J. Dudek and W. Plóciennik, *Phys. Rev. Lett.* **93**, 052501 (2004).
- [38] P. Olbratowski, J. Dobazewski and J. Dudek, *Phys. Rev. C* **73**, 054308 (2006).
- [39] D. Almeded and S. Frauendorf, arXiv:0709.0969v1 [nucl-th] (2007).
- [40] J. Peng, J. Meng, S. Q. Zhang, *Phys. Rev. C* **68**, 044324 (2003).
- [41] J. Peng, J. Meng, S. Q. Zhang, *Chin. Phys. Lett.* **20**, 1223 (2003).
- [42] T. Koike, K. Starosta and I. Hamamoto, *Phys. Rev. Lett.* **93**, 172502 (2004).
- [43] S. Q. Zhang, B. Qi, S. Y. Wang, and J. Meng, *Phys. Rev. C* **75**, 044307 (2007).
- [44] S. Y. Wang, S. Q. Zhang, B. Qi and J. Meng, *Phys. Rev. C* **75**, 024309 (2007).
- [45] S. Y. Wang, S. Q. Zhang, B. Qi, J. Peng, J. M. Yao, and J. Meng, *Phys. Rev. C* **77**, 034314 (2008).
- [46] B. Qi, S. Q. Zhang, J. Meng, S. Y. Wang, and S. Frauendorf, *Phys. Lett. B* **675**, 175 (2009).
- [47] B. Qi, S. Q. Zhang, S. Y. Wang, J. M. Yao, and J. Meng, *Phys. Rev. C* **79**, 041302(R) (2009).
- [48] K. Higashiyama, N. Yoshinaga and K. Tanabe, *Phys. Rev. C* **72**, 024315 (2005).
- [49] D. Tonev *et al.*, *Phys. Rev. C* **76**, 044313 (2007).

- [50] S. Brant, D. Tonev, G. de Angelis, and A. Ventura, *Phys. Rev. C* **78**, 034301 (2008).
- [51] S. Brant and C. M. Petrache, *Phys. Rev. C* **79**, 054326 (2009).
- [52] Ch. Droste, S.G. Rohoziński, K. Starosta, L. Próchniak, and E. Grodner, *Eur. Phys. J. A* **42**, 79C89 (2009).
- [53] J. Meng, J. Peng, S. Q. Zhang and S.-G. Zhou, *Phys. Rev. C* **73**, 037303 (2006).
- [54] J. Peng, H. Sagawa, S. Q. Zhang, J. M. Yao, Y. Zhang, and J. Meng, *Phys. Rev. C* **77**, 024309 (2008).
- [55] J. M. Yao, B. Qi, S. Q. Zhang, J. Peng, S. Y. Wang, and J. Meng, *Phys. Rev. C* **79**, 067302 (2009).
- [56] J. Meng, S.Q. Zhang, B.Qi and S.Y. Wang, XVIII International School on Nuclear Physics, neutron physics, and applications, Varna, Bulgaria, to be appeared in *J. Phys. Conference Series* (2010).
- [57] W. Koepf and P. Ring, *Nucl. Phys. A* **493**, 61 (1989).
- [58] A. V. Afanasjev, P. Ring and J. König, *Nucl. Phys. A* **676**, 196 (2000).
- [59] H. Madokoro, J. Meng, M. Matsuzaki and S. Yamaji, *Phys. Rev. C* **62**, 061301(2000).
- [60] J. Peng, J. Meng, P. Ring and S. Q. Zhang, *Phys. Rev. C* **78**, 024313 (2008).
- [61] A. Klein, *Phys. Rev. C* **63**, 014316 (2000), and references therein.
- [62] A. Bohr and B. R. Mottelson, *Nuclear Structure* (Benjamin, New York, 1975), Vol. 2.
- [63] P. Ring and P. Shuck, Nuclear Many body problem, 1981.
- [64] Y.S. Chen and Z.C. Gao, *High Energy Phys. & Nucl. Phys.* **30**, 14 (2006).
- [65] A. Arima, M. Harvey and K. Shimizu, *Phys. Lett. B* **30**, 517 (1969).
- [66] K.T. Hecht and A. Adler, *Nucl. Phys.* **A137**, 129 (1969).
- [67] J.N. Ginocchio, *Phys. Rev. Lett.* **78** 436, (1997).
- [68] J. Meng, K. Sugawara-Tanabe, S. Yamaji, P. Ring and A. Arima, *Phys. Rev. C* **58**, R628 (1998).
- [69] J. Meng, K. Sugawara-Tanabe, S. Yamaji and A. Arima, *Phys. Rev. C* **59**, 154 (1999).
- [70] T.S. Chen, H.F. Lü, J. Meng, S.Q. Zhang and S.G. Zhou, *Chin. Phys. Lett.* **20**, 358 (2003).
- [71] J. Y. Zeng, J. Meng, C. S. Wu, E. G. Zhao, Z. Xing, and X. Q. Chen, *Phys. Rev. C* **44**, R1745 (1991).
- [72] Q. Xu *et.al.*, *Phys. Rev. C* **78**, 064301 (2008).
- [73] C. M. Petrache et al., *Phys. Rev. C* **65**, 054324 (2002).
- [74] M. A. Cardona et al., *Phys. Rev. C* **55**, 144 (1997).
- [75] P. Petkov, P. vonBrentano, J. Jolie, and R. V. Jolos, *Phys. Rev. C* **76**, 044318 (2007).
- [76] K. Hara and S. Iwasaki, *Nucl. Phys. A* **332**, 61 (1979).
- [77] K. Hara and Y. Sun, *Int. J. Mod. Phys. E* **4**, 637 (1995).
- [78] J.A. Sheikh and K. Hara, *Phys. Rev. Lett.* **82**, 3968 (1999).
- [79] Z.C. Gao, Y.S. Chen and Y. Sun, *Phys. Lett. B* **634**,195 (2006).
- [80] J.A. Sheikh, G.H. Bhat, Y. Sun, G.B. Vakil, and R. Palit, *Phys. Rev. C* **77**, 034313 (2008).
- [81] A. Valor, P.-H. Heenen, and P. Bonche, *Nucl. Phys.* **A671**, 145 (2000).
- [82] R. Rodríguez-Guzmán, J. L. Egido, and L. M. Robledo, *Phys. Rev. C* **65**, 024304 (2002).
- [83] R. Rodríguez-Guzmán, J. L. Egido, and L. M. Robledo, *Nucl. Phys. A* **709**, 201 (2002).
- [84] T. Nikšić, D. Vretenar, and P. Ring, *Phys. Rev. C* **73**, 034308 (2006).
- [85] T. Nikšić, D. Vretenar, and P. Ring, *Phys. Rev. C* **74**, 064309 (2006).
- [86] D. Baye and P.-H. Heenen, *Phys. Rev. C* **29**, 1056 (1984).
- [87] H. Zduńczuk, W. Satula, J. Dobaczewski, and M. Kosmowski, *Phys. Rev. C* **76**, 044304 (2007).
- [88] M. Bender and P.-H. Heenen, *Phys. Rev. C* **78**, 024309 (2008).
- [89] J.M. Yao, J. Meng, P. Ring, and D. Pena Arteaga , *Phys. Rev. C* **79**, 044312 (2009).
- [90] J.M. Yao, J. Meng, P. Ring, and D. Vretenar, arXiv:0912.2650v1 [nucl-th] (2009).
- [91] T. Nikšić, Z.P. Li, D. Vretenar, L. Próchniak, J. Meng and P. Ring, *Phys. Rev. C* **79**, 034303 (2009).
- [92] Z.P. Li, T. Nikšić, D. Vretenar, J. Meng, G.A. Lalazissis and P. Ring, *Phys. Rev. C* **79**, 054301 (2009).
- [93] Z. P. Li, T. Nikšić, D. Vretenar and J. Meng, *Phys. Rev. C* **80**, 061301(R) (2009).